(IJC)

ISSN 2307-4523 (Print & Online)



http://ijcjournal.org/

# Design of MIMO Antenna Array Architecture for Higher Channel Capacity

Phyu Phyu Thin[a]*, Aung Myint Aye[b]

[a]*Department of Information Technology, Mandalay Technological University, Mandalay, The Republic of the Union of Myanmar*

[b] *Department of Information Technology, Mandalay Technological University, Mandalay, The Republic of the Union of Myanmar*

[a]*Email: phyuphyu285@gmail.com*

[b]*Email: dr.aungmyintaye@gmail.com*

**Abstract**

In many extensive researches, the channel capacity of narrowband multiple-input multiple-output (MIMO) communication systems in indoor Line-of-Sight (LOS) environment is investigated and proved that the LOS signal can get the high channel capacity by designing the antenna arrays. On the other hand, MIMO systems offer significant capacity enhancements in non Line-of-Sight (LOS) environments where rich scattering is present. However, the wireless propagation mechanisms and antenna array orientation should be considered when designing the wireless network to get more precise results and improve the performance. This paper investigates the performance of MIMO system based on two ray ground reflection model. In this system, the LOS signal and the LOS signal with one ground reflected ray can provide the optimum MIMO capacity performance if specific designed antenna arrays are employed at both sides of the communications link. For achieving the optimal MIMO capacity in a LOS environment, the antenna array architecture is considered as a function of the distance between transmitter and receiver, the transmitted and received antennas' height, the array orientation and the antenna spacing distance. The capacity sensitivity for a number of MIMO architectures with respect to the experimental data and simulation is investigated by using MATLAB programming language.

***Keywords:*** MIMO; channel capacity; indoor propagation; antenna array orientation; two ray ground reflection model.

---

* Corresponding author

## 1. Introduction

MIMO wireless communication systems can increase channel capacity greatly without the expansion of bandwidth by applying space diversity at both transmit and receive antennas. MIMO capacity increases linearly with the number of antennas, whereas Single-Input Single-Output (SISO), Single-Input Multiple-Output (SIMO) and Multiple-Input Single-Output (MISO) systems all increase only logarithmically [1]. Multiple antenna systems also mitigate deep fades on any of the channel by the spatial diversity provided by multiple spatial paths. Each pair of transmit-receive antennas provides a signal path from transmitter to receiver. By sending the same information through different paths, multiple independently-faded replicas of the data symbol can be obtained at the receiving end and hence, more reliable reception is achieved. Capacity increases linearly with Signal-to-Noise Ratio (SNR) at low SNR, but increases logarithmically with SNR at high SNR [2].

For LOS channels, ray tracing method is used to find array geometries which result in channel matrices with close to nonnegligible eigenvalues. The LOS channel response will change as the receiver is moved, so that a capacity distribution is obtained from the ensemble of sample matrix elements at different receiver locations [3].

However, the capacity is practically affected by various channel parameters, especially correlation between subchannels. Many models representing MIMO channels have been published, but most of the models assume specific scenarios, and cannot consider sufficiently various parameters to affect channel performance [2]. According to the ray tracing method, the method proposed here can consider different types of antenna patterns with array orientation and ground reflected ray of each path between transmit (Tx) and receive (Rx) antenna.

The objective of this paper is to design a new geometrical model for the LOS component with regard to capacity as a function of the distance between transmitter and receiver, the transmitted and received antennas' height, the array orientation and the antenna spacing distance and ground reflected ray for each path at the carrier frequency of 2.4 GHz.

## 2. Background Theory

### *2.1. Two Ray Ground Reflection Model*

In a wireless communication system, if there is only a single direct path between transmitter and receiver, the Friis free space propagation model can be used for simple path loss estimations. However, a slightly more realistic model, two-ray model is a commonly used propagation model because it accounts for a ground-reflected path between transmitter and receiver in addition to the LOS component as shown in Figure 1.

Two-ray model has been shown to produce more accurate path loss estimates at long distances than Friis free space equation. It accounts for antenna height differences at the transmitter and receiver, which is not considered in the Friis equation [4]. The two-ray model also assumed that the angle of incidence of the reflected ray becomes almost grazing at large distance, which leads to a reflection coefficient of -1 [5].

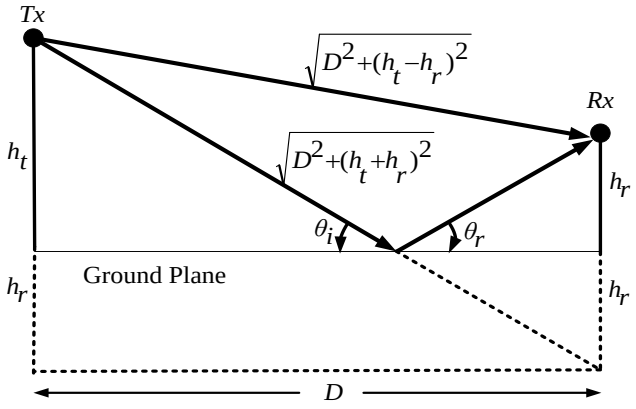


**Figure 1:** Two ray ground reflection model with not equal Tx and Rx antenna heights

### *2.2. MIMO Channel Model*

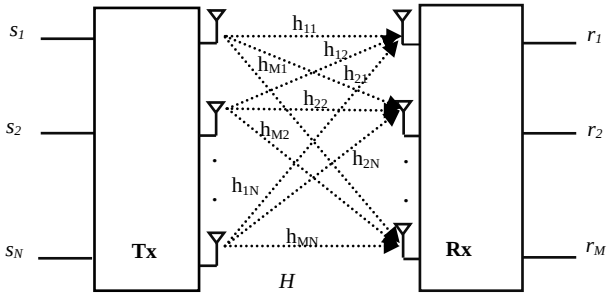


**Figure 2:** The diagram of a MIMO system

A single user MIMO system employs $N$ antennas at the transmitter and $M$ antennas at the receiver when transmitting data over a channel as shown in Figure 2. The received signal in each symbol period is represented by $M\times1$ received complex-valued signal vector, $r$ and the transmitted signal is represented by the $N\times1$ transmitted complex-valued signal vector, $s$. The channel $H$ is described by an $M \times N$ complex matrix where the $ji^{th}$ component of the matrix $H$, denoted by $h_{ji}$, is the channel response between the $j^{th}$ received antenna and the $i^{th}$ transmitted antenna. The additive white Gaussian noise at the receiver is described by an $M \times 1$ column matrix $n$. Thus, the narrowband frequency flat fading MIMO channel model is described by the matrix equation as [6]:

$$r = Hs + n \tag{1}$$

The $M \times N$ MIMO channel matrix can be expressed as follows:

$$H = \begin{bmatrix} h_{11} & h_{12} & \dots & h_{1N} \\ h_{21} & h_{22} & \dots & h_{2N} \\ \dots & \dots & \dots & \dots \\ h_{M1} & h_{M2} & \dots & h_{MN} \end{bmatrix} \tag{2}$$

### *2.3. MIMO Channel Capacity*

Acquiring channel knowledge at the transmitter is in general very difficult in practical systems. When the transmitter has no channel state information, it is optimal to evenly distribute the transmitted power among the transmit antennas. The MIMO channel capacity with this scenario can be written as [7]:

$$C = \log_2 \det[I_M + \frac{P_t}{N\sigma_n^2} HH^H] bps/Hz \quad (3)$$

Where $I_M$ is the $M \times M$ identity matrix, det denotes the determinant, $P_t$ is the total average transmitted power from all Tx antennas, $\sigma^2_n$ is the noise variance (power) of the receiving system and $H^H$ is the Hermitian transpose operation of $H$, i.e. the conjugate transpose of complex matrix $H$. In the following, it is also assumed that the average total power $P_r$ received by each Rx antenna (regardless of noises) is equal to the average total transmitted power $P_t$ from all Tx antennas, the SNR at each Rx antenna is then

$$\rho = \frac{P_r}{\sigma_n^2} \quad (4)$$

By applying singular value decomposition (SVD) to $H$ [8], equation (3) can be decomposed as:

$$C = \sum_{i=1}^{m} \log_2(1 + \frac{\rho}{N}\lambda_i) bps/Hz \quad (5)$$

Where, $\lambda_i$ is the $i^{th}$ eigenvalue of $HH^H$ and this equation shows that a MIMO system can be viewed as consisting of $m$ = min ($M$, $N$) parallel SISO channels, where each channel has gain $\lambda_i$, and an average SNR downscaled with the number of transmitters compared to a SISO system with the same total transmitted power.

## 3. LOS MIMO Channel with Array Orientation and Ground Reflection

A MIMO channel with direct LOS paths between the antennas is assumed and both Tx and Rx antennas are in linear arrays as shown in Figure 3. The antenna separation is denoted by $d_t$ and $d_r$ for both Tx and Rx antennas respectively and the distance between each Tx and Rx antenna by $d_{ji}$ ($j=1,\ldots,M$, $i=1,\ldots,N$). $D$ is the distance between transmitter and receiver. The height of Tx and Rx antennas are $h_t$, and $h_r$ respectively and $h_t=h_r = a_h + b_h$, where, $a_h = t \sin(\theta_t)$ and $t \sin(\theta_r)$ for Tx and Rx antenna respectively and $b_h$ is the height of the base under the antenna.

The proposed system is concentrated on the pure LOS channel and there is no any obstructed thing between Tx and Rx antenna. Moreover, people are not allowed to walk during experiments. In [3], it was shown that by placing the antennas in a MIMO system in a smart way, the pure LOS channel matrix actually becomes high rank, which corresponds to many nonzero eigenvalues $\lambda_i$ and thus high MIMO capacity. In this system, more general geometry, using both Tx and Rx array arbitrary orientation and ground reflection for each path is considered.

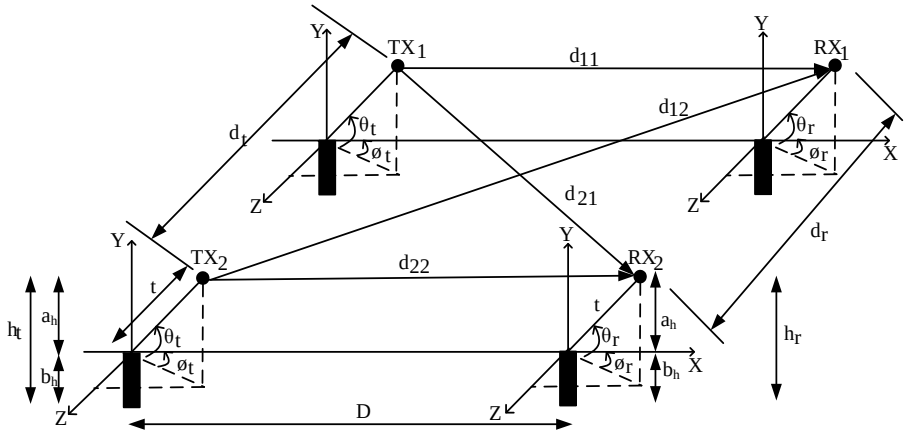


**Figure 3:** 2 × 2 LOS channel with Tx and Rx array orientation

In this system, the *x*-axis is taken to be in the direction from each Tx antenna array to each Rx antenna array and the z-axis is taken to be in the direction between each Tx antenna and each Rx antenna [9]. The transmit array is placed in the *x, y* plane. In reference [10], the antenna spacing distances, $d_t$ and $d_r$ with the uniform linear array (ULA) are constant. However, the system parameters, $d_t$, $d_r$, $h_t$, $h_r$ and $D$ can take different values in this proposed system. The total length of the Tx and Rx arrays are denoted by $(N-1)\,d_t$ and $(M-1)\,d_r$ and the angles $\theta_t$, $\Phi_t$, $\theta_r$ and $\Phi_r$ are the rotation angles of the local spherical coordinate system at the transmitter and receiver respectively.

### *3.1. Evaluation of Distance between each Tx and Rx Antenna*

The technique used in this proposed system is based on ray tracing approach. The index of Rx and Tx antennas are described by $j = 1,\ldots, M$, and $i = 1,\ldots, N$ respectively. As in reference [11], the antenna placements for Tx and Rx antenna at *x, y* and *z* coordinates are given as follows:

$$Tx_i[x,y,z]=[(i-1)d_t\cos(\theta_t)\cos(\phi_t)]_x,[(i-1)d_t\sin(\theta_t)]_y,[(i-1)d_t\cos(\theta_t)\sin(\phi_t)]_z \tag{6}$$

$$Rx_j[x,y,z]=[D+(j-1)d_r\cos(\theta_r)\cos(\phi_r)]_x,[(j-1)d_r\sin(\theta_r)]_y,[(j-1)d_r\cos(\theta_r)\sin(\phi_r)]_z \tag{7}$$

By using the Euclidean distance formula, the distance between each Tx and Rx antenna is given by

$$d_{ji}=[(D+(j-1)d_r\cos(\theta_r)\cos(\phi_r)-(i-1)d_t\cos(\theta_t)\cos(\phi_t))^2+((j-1)d_r\sin(\theta_r)-(i-1)d_t\sin(\theta_t))^2+ ((j-1)d_r\cos(\theta_r)\sin(\phi_r)-(i-1)d_t\cos(\theta_t)\cos(\phi_t))^2]^{1/2} \tag{8}$$

By assuming that $(D+(j-1)d_r\cos(\theta_r)\cos(\phi_r)-(i-1)d_t\cos(\theta_t)\cos(\phi_t))\approx D$ and using the approximation $\sqrt{A^2+B}\approx A+\frac{B}{2A}$ if A >> B since the distance $D$ is much larger than the antenna spacing distance, $d_t$ and $d_r$, the equation (8) can be written as:

$$d_{ji} \approx (D + (j-1)d_r \cos(\theta_r)\cos(\phi_r) - (i-1)d_t \cos(\theta_t)\cos(\phi_t)) + \frac{1}{2D}[((j-1)d_r \sin(\theta_r) - (i-1)d_t \sin(\theta_t))^2 + ((j-1)d_r \cos(\theta_r)\sin(\phi_r) - (i-1)d_t \cos(\theta_t)\cos(\phi_t))^2] \quad (9)$$

### *3.2. Channel Matrix Estimation*

The channel matrix $H$ is modeled using a ray-tracing approach that includes LOS paths and ground reflected rays for each path as shown in Figure 4.

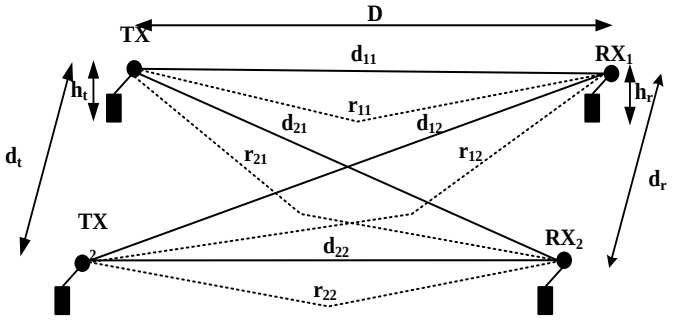


**Figure 4:** 2 × 2 LOS channel with ground reflection

Reflection attenuation of the reflected waves is disregarded in this proposed system due to the path loss and reflection loss they incur, as well as the array orientation to be considered. For narrowband communication system, the channel is modeled as

$$H = H_{LOS} + H_R \quad (10)$$

Where $H_{LOS}$, and $H_R$ are the contributions of the LOS path with both Tx and Rx array orientation and ground reflected path, respectively. In LOS condition, the phase of each channel gain, $h_{ji}(LOS)$ is a function of the geometry and carrier frequency [11]. Thus, the channel gain, $h_{ji}(LOS)$, which is $ji^{th}$ entry of $H_{LOS}$, representing the complex gain from $j^{th}$ Rx antenna to $i^{th}$ Tx antenna is given by

$$h_{ji}(LOS) = \exp(\frac{-j2\pi d_{ji}}{\lambda}) \quad (11)$$

Where $\lambda$ is the wavelength of the carrier frequency and $d_{ji}$ is the LOS path between the $j^{th}$ Rx antenna and $i^{th}$ Tx antenna obtained by equation (9). The channel gain, $h_{ji}(R)$, from the $j^{th}$ Rx antenna to $i^{th}$ Tx antenna is given by

$$h_{ji}(R) = \exp(\frac{-j2\pi r_{ji}}{\lambda}) \quad (12)$$

Where $r_{ji}$ is the ground reflected path for each LOS path between the $j^{th}$ Rx antenna and $i^{th}$ Tx antenna.

## 4. Experimental Setup

The experimental procedures for this proposed system are briefly described with the system block diagram in Figure 5. All the experiments were carried out at the portico of the Mandalay Technological University, the Republic of the Union of Myanmar. The building layout and the top view of the portico are shown in Figure 6 and Figure 7. TP-Link TL-WR1043N router with two 8 dBi omnidirectional antennas was used as a transmitter and TP-Link TL-WN722N 150 Mbps wireless adapter, configured to mount two 8 dBi omnidirectional antennas was used as a receiver in all experiments. In all experiments, the actual on-site signal strength measurement readings were taken using signal analyser software called inSSIDer, which was installed in a laptop. The carrier frequency was 2.4 GHz and the transmitted power level 20 dBm was used during measurements.

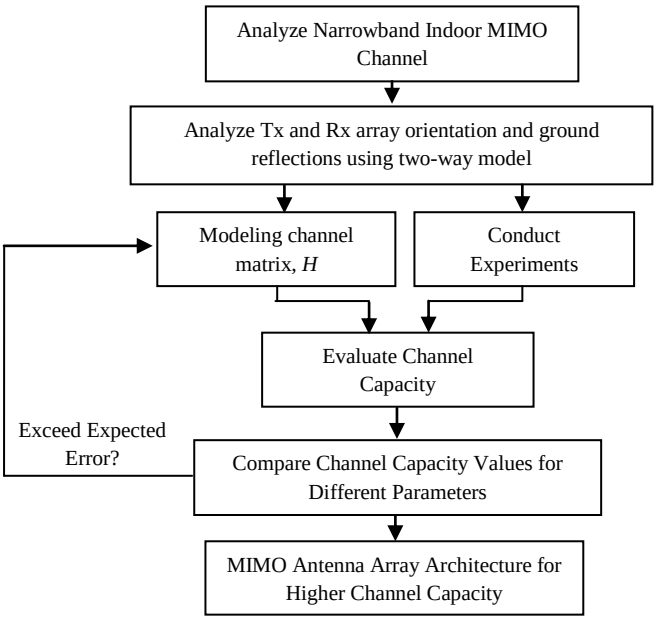


**Figure 5:** Block diagram of proposed System

**Figure 6:** Building layout

All the experimental points were marked at the center of the portico as one meter from one end of the portico to the other end and both Tx and Rx antennas are positioned with the spherical coordinates before measuring the experiments. Moreover, there was no movement of Tx and Rx antennas during measurements.

To estimate the channel attenuation and variations, the experiments were made by moving the receiver at every one meter while the placement of transmitter was stable. The experimental record photos of this system are shown in Figure 8.

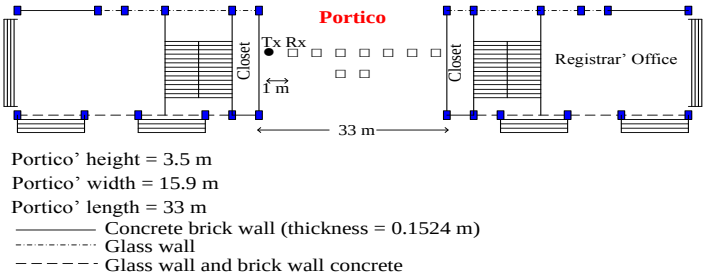


**Figure 7:** Top view of the portico

**Figure 8:** Placement of transmitter and receiver in the portico

## 5. Performance Analysis

The configuration for this proposed system is based on the angles of the local spherical coordinate system at the transmitter and receiver $\theta_t$, $\Phi_t$ and $\theta_r$, $\Phi_r$ respectively. The capacity performance of MIMO antenna structures is compared using the special angles, $0^\circ$, $30^\circ$, $45^\circ$,$60^\circ$ and $90^\circ$ for $\theta_t$ and $\theta_r$ and $90^\circ$ for $\Phi_t$ and $\Phi_r$ respectively. The performance comparison is shown with the channel capacity versus signal-to-noise ratio (SNR) at 50 dB in the following Table 1.

Figure 9 shows the experimental result for 2 × 2 LOS MIMO system using array orientation angles of $\theta_t = \theta_r = \Phi_t = \Phi_r = 90^\circ$ and antenna spacing distances of $d_t = d_r = 0.5$ m and 0.1524 m respectively. The proposed system with angles $\theta_t = \theta_r = \Phi_t = \Phi_r = 90^\circ$ has the same consideration with the system which does not have Tx and Rx antenna orientations [12]. However, it can be seen that the results with Tx and Rx array orientation have higher channel capacity than the results with no antenna orientations. This is because of the calculation of the distance between each Tx and Rx antenna corresponding to the antenna array orientation.

**Table 1:** Comparison Results for Proposed System

| Signal-to-Noise Ratio (SNR) | Tx Orientation Angles | | Rx Orientation Angles | | Channel Capacity (bps/Hz) without GR | Channel Capacity (bps/Hz) with GR ($h_t$=$h_r$ =1m) | Channel Capacity (bps/Hz) with GR ( $h_t$ =3m> $h_r$ =1m |
|---|---|---|---|---|---|---|---|
| | $\theta_t$ | $\Phi_t$ | $\theta_r$ | $\Phi_r$ | | | |
| 50 dB | 0° | 90° | 0° | 90° | 28.5692 | 27.5969 | 21.3715 |
| | 30° | 90° | 30° | 90° | 29.1911 | 30.0925 | 32.1012 |
| | 45° | 90° | 45° | 90° | 29.0435 | 33.0110 | 30.6023 |
| | 60° | 90° | 60° | 90° | 28.6348 | 17.0495 | 29.4203 |
| | 90° | 90° | 90° | 90° | 29.0883 | 33.0035 | 29.7210 |

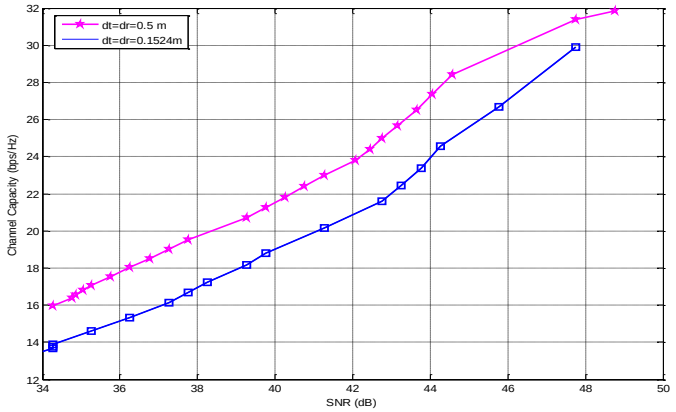


**Figure 9:** Channel capacity versus SNR for LOS channel using $\theta_t = \theta_r = \Phi_t = \Phi_r = 90^\circ$

In the following, the simulation results for a 2×2 system at $D$ = 24 m, SNR, $\rho$ = 1 to 50 dB, $h_t = h_r$=1m for equal height, $h_t$ = 1m or 3m and $h_r$= 1m or 3m for not equal height, and the antenna spacing distance, $d_t = d_r$ = 0.5m are described. Figure 10 shows the channel capacity versus SNR for three different channels, LOS channel without ground reflection, GR, LOS channel with GR for equal Tx and Rx heights ($h_t = h_r$) and LOS channel with GR for not equal Tx and Rx heights ($h_t > h_r$ or $h_r > h_t$) using all the orientation angles of 90°. From this figure, it can be seen how the channel capacity for three different channels differ when the SNR increases with the antenna configuration $\theta_t = \theta_r = \Phi_t = \Phi_r = 90^\circ$. The channel capacity for LOS channel with GR ($h_t = h_r$) is higher than any two channels with this antenna configuration. The antenna configuration with $\theta_t = \theta_r = 45^\circ$, $\Phi_t = \Phi_r = 90^\circ$ has the similar result as shown in Figure 11.

The comparison result for LOS channel and LOS channel with ground reflection (GR) using $\theta_t = \theta_r = 0^\circ$ and $\Phi_t = \Phi_r = 90^\circ$ is plotted in Figure 12. In this figure, LOS channel without GR has higher capacity result, but it is lower than the results of LOS channel with GR ($h_t = h_r$) in Figure 10 and Figure 11.

On the other hand, in this array configuration, the capacity for LOS channel with GR ($h_t > h_r$ or $h_r > h_t$) is significantly lower than any other results.

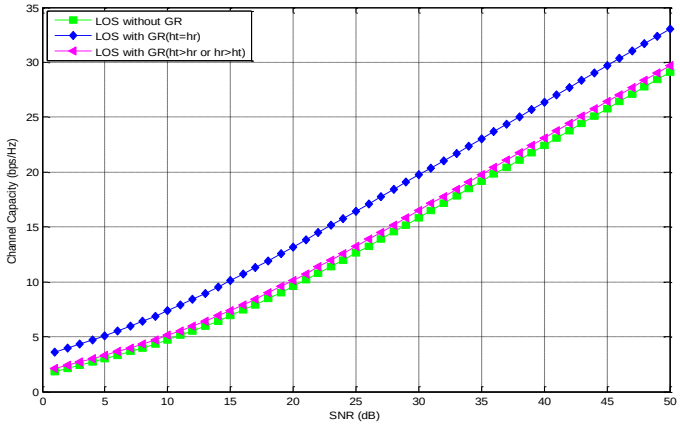


**Figure 10:** Channel capacity versus SNR for LOS channel and LOS channel with Ground Reflection (GR) using $\theta_t = \theta_r = \Phi_t = \Phi_r = 90^\circ$

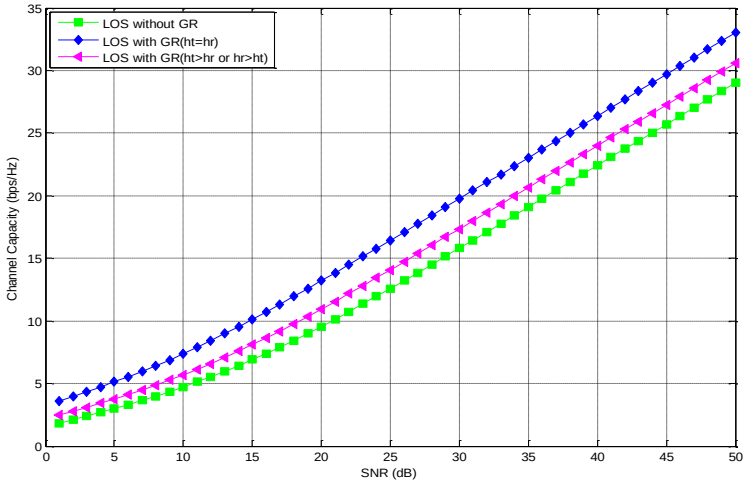


**Figure 11:** Channel capacity versus SNR for LOS channel and LOS channel with Ground Reflection (GR) using $\theta_t = \theta_r = 45^\circ$, $\Phi_t = \Phi_r = 90^\circ$

The following figures, Figure 13 and Figure 14 show the results for the antenna configurations of $\theta_t = \theta_r = 30^\circ$, $\Phi_t = \Phi_r = 90^\circ$ and $\theta_t = \theta_r = 60^\circ$, $\Phi_t = \Phi_r = 90^\circ$ respectively. By seeing these results, it confirms that the antenna configurations with $\theta_t = \theta_r = 90^\circ$, $\Phi_t = \Phi_r = 90^\circ$ and $\theta_t = \theta_r = 45^\circ$, $\Phi_t = \Phi_r = 90^\circ$ are the best antenna structure for LOS channel with ground reflection, GR ($h_t = h_r$) and the antenna configuration with $\theta_t = \theta_r = 30^\circ$, $\Phi_t = \Phi_r = 90^\circ$ is the best antenna structure for LOS channel with ground reflection, GR ($h_t > h_r$ or $h_r > h_t$). This is because of the contributions of this proposed system and so Tx and Rx antenna configuration at the coordinates *x*, *y* and *z* is the well-designed antenna configuration and ground reflection between each Tx and Rx antennas should be considered.

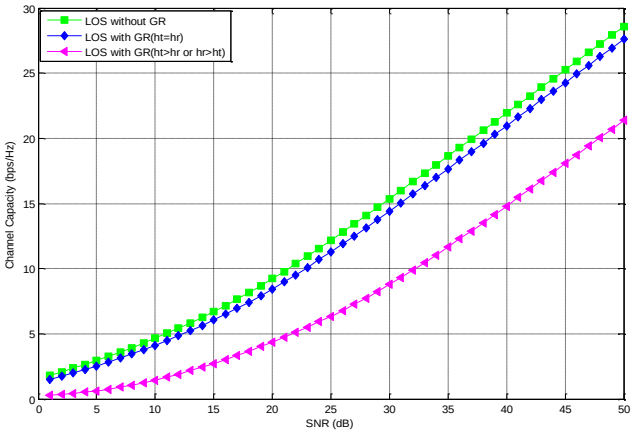


**Figure 12:** Channel capacity versus SNR for LOS channel and LOS channel with Ground Reflection (GR) using $\theta_t = \theta_r = 0^\circ$, $\Phi_t = \Phi_r = 90^\circ$

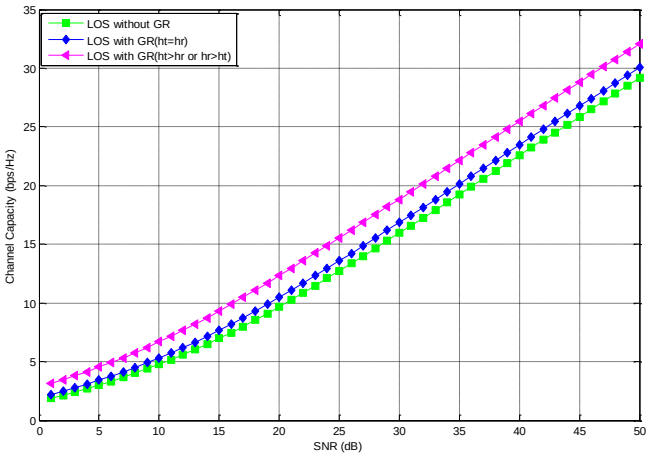


**Figure 13:** Channel capacity versus SNR for LOS channel and LOS channel with Ground Reflection (GR) using $\theta_t = \theta_r = 30^\circ$, $\Phi_t = \Phi_r = 90^\circ$

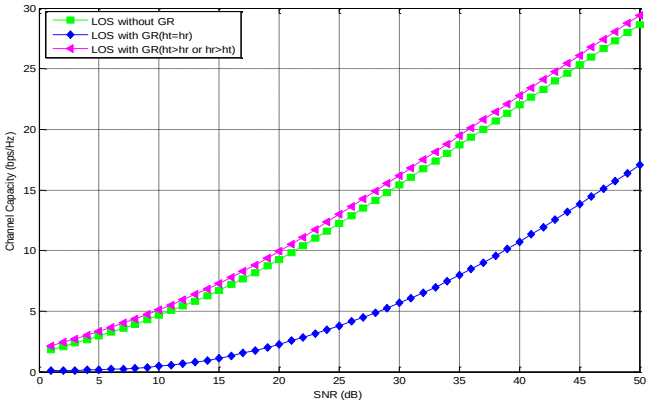


**Figure 14:** Channel capacity versus SNR for LOS channel and LOS channel with Ground Reflection (GR) using $\theta_t = \theta_r = 60^\circ$, $\Phi_t = \Phi_r = 90^\circ$

## 6. Conclusion

A new LOS MIMO model is designed geometrically with the consideration of the ground reflection for each path to find the optimal antenna array orientation with regard to higher channel capacity. The experiments were made for 2×2 LOS channel using $\theta_t = \theta_r = \Phi_t = \Phi_r = 90^\circ$ antenna configurations. However, the simulation analysis was made for other antenna configurations using the special angels of $0^\circ$, $30^\circ$, $45^\circ$, $60^\circ$ and $90^\circ$ for $\theta_t$ and $\theta_r$ and $90^\circ$ for $\Phi_t$ and $\Phi_r$ respectively. The antenna configuration with $\theta_t = \theta_r = 90^\circ$, $\Phi_t = \Phi_r = 90^\circ$ and $\theta_t = \theta_r = 45^\circ$, $\Phi_t = \Phi_r = 90^\circ$ can get higher channel capacity than any other configuration for LOS channel with ground reflection, GR ($h_t = h_r$) and the antenna configuration with $\theta_t = \theta_r = 30^\circ$, $\Phi_t = \Phi_r = 90$ can give higher channel capacity result for LOS channel with ground reflection, GR ($h_t > h_r$ or $h_r > h_t$).

In addition, only 2 x 2 matrix antennas radiation type can be used in all experiments as this system proposed to design the antenna array architecture for higher channel capacity and this system can be extended by using more antennas similarly. This proposed system can be applied in the consideration of the antenna array architecture in narrowband communication system.

## 7. Further Extension

As the further extension, other channel performance measures will be used to analyze the array geometry. Other types of routers, wireless adapters, antennas, signal analyzer machines or analyzer software will be used to make performance comparison and estimate the better results. In addition, reflective paths from the side walls and roof will be considered. The experiments in different indoor environments at Mandalay Technological University will also be conducted.

## Acknowledgements

The author especially would like to take this opportunity to express my sincere gratitude, respect and regards for supervisor Dr. Aung Myint Aye, Associate Professor, Head of the Department of Information Technology, Mandalay Technological University, Mandalay, Mandalay Division, the Republic of the Union of Myanmar under whose guidance, constant encouragement, patient and trust, I have worked on this paper. And the author is thankful to all my friends who have directly or indirectly assisted me in my endeavors.

## References

[1] Charan Langton and Bernard Sklar. “Tutorial 27 - Finding MIMO,” Oct. 2011.

[2] Daniel W. Bliss and Keith W. Forsythe. “MIMO Environmental Capacity Sensitivity,” MIT Lincoln Laboratory, Lexington, Massachusetts.

[3] P. F. Driessen and G. J. Foschini. “On the Capacity Formula for Multiple Input–Multiple Output Wireless Channels: A Geometric Interpretation,” IEEE Transactions on Communications, vol. 47, No. 2, Feb. 1999.

[4] Julia Andrusenko, Jack Burbank, and Jon Ward. "Modeling and Simulation for RF Propagation," Dec. 2009.

[5] Khaing Phyu and Aung Myint Aye."Modelling and Analyzing the Signal Strength Attenuation for Indoor Radio Wave Propagation," Department of Information Technology, Mandalay Technological University, the Republic of the Union of Myanmar, May 2011.

[6] A. J. Paulraj, D. Gore, and R. U. Nabar. "Performance limits in fading MIMO channels," Globecome, 2002.

[7] G. J. Foschini and M. J. Gans, "On limits of wireless communication in a fading environment when using multiple antennas," *Wireless Personal Commun.*, vol. 6, no. 3, pp. 311–335, Mar. 1998.

[8] Stefan Schindler and Heinz Mellein. "Accessing a MIMO Channel," Rohde & Schwarz, Available: http://www.rohde-schwarz.com [Feb. 2011].

[9] I. Sarris and A. Nix. "Design and performance assessment of maximum capacity MIMO architectures in line-of-sight," IEE Proc.-Commun., Vol. 153, No. 4, Aug. 2006.

[10] Frode Bøhagen, P°al Orten and Geir E. Øien. "Construction and Capacity Analysis of High-Rank Line-of-Sight MIMO Channels," UniK/Nera Research, Bergerveien 12, N-1375 Billingstad, Norway, 2005.

[11] Phyu Phyu Thin and Aung Myint Aye. "Indoor MIMO Channel Capacity Prediction in Line-of-Sight (LOS) Environment," the Fifth International Conference on Science and Engineering (ICSE 2014), Dec. 29-30, 2014, Yangon, Myanmar.